Molecular & Biochemical Parasitology 200 (2015) 9–18

Contents lists available at ScienceDirect

Molecular & Biochemical Parasitology

In vitro metacyclogenesis of *Trypanosoma cruzi* induced by starvation correlates with a transient adenylyl cyclase stimulation as well as with a constitutive upregulation of adenylyl cyclase expression

Afsaneh Hamedi[a], Larisse Botelho[b], Constança Britto[b], Stenio Perdigão Fragoso[f], Adriana Castilhos Souza Umaki[c], Samuel Goldenberg[f], Guy Bottu[e], Didier Salmon[d,*]

[a] *Fiocruz, Instituto Oswaldo Cruz, Av. Brasil 4365, 21040-900 Rio de Janeiro, RJ, Brazil*
[b] *Laboratório de Biologia Molecular e Doenças Endêmicas, Instituto Oswaldo Cruz, Fiocruz, Av. Brasil 4365, 21040-900 Rio de Janeiro, Brazil*
[c] *Instituto Carlos Chagas, Fiocruz, PR, Rua Professor Algacyr Munhoz Mader 3775, Curitiba 81350-010, PR, Brazil*
[d] *Institute of Medical Biochemistry Leopoldo de Meis, Centro de Ciências e da Saúde, Federal University of Rio de Janeiro, Av. Brigadeiro Trompowsky, Rio de Janeiro 21941-590, Brazil*
[e] *Université Libre de Bruxelles, Campus de la Plaine, Boulevard du Triomphe, 1050 Brussels, Belgium*
[f] *Instituto de Biologia Molecular do Paraná, Rua Professor Algacyr Munhoz Mader 3775, Curitiba 81350-010, PR, Brazil*

ARTICLE INFO

Article history:
Received 28 November 2014
Received in revised form 10 April 2015
Accepted 15 April 2015
Available online 23 April 2015

Keywords:
T. cruzi
Metacyclogenesis
cAMP
Adenylyl cyclase
Parasite differentiation

ABSTRACT

The *Trypanosoma cruzi* adenylyl cyclase (AC) multigene family encodes different isoforms (around 15) sharing a variable large N-terminal domain, which is extracellular and receptor-like, followed by a transmembrane helix and a conserved C-terminal catalytic domain. It was proposed that these key enzymes in the cAMP signalling pathway allow the parasite to sense its changing extracellular milieu in order to rapidly adapt to its new environment, which is generally achieved through a differentiation process. One of the critical differentiation events the parasitic protozoan *T. cruzi* undergoes during its life cycle, known as metacyclogenesis, occurs in the digestive tract of the insect and corresponds to the differentiation from noninfective epimastigotes to infective metacyclic trypomastigote forms. By *in vitro* monitoring the activity of AC during metacyclogenesis, we showed that both the activity of AC and the intracellular cAMP content follow a similar pattern of transient stimulation in a two-step process, with a first activation peak occurring during the first hours of nutritional stress and a second peak between 6 and 48 h, corresponding to the cellular adhesion. During this differentiation process, a general mechanism of upregulation of AC expression of both mRNA and protein is triggered and in particular for a major subclass of these enzymes that are present in various gene copies commonly associated to the *THT* gene clusters. Although the scattered genome distribution of these gene copies is rather unusual in trypanosomatids and seems to be a recent acquisition in the evolution of the *T. cruzi* clade, their encoded product redistributed on the flagellum of the parasite upon differentiation could be important to sense the extracellular milieu.

1. Introduction

The molecular mechanisms used by parasites to undergo developmental transformations and adapt to their hosts are poorly characterized. This is true for the unicellular protozoan parasite *Trypanosoma cruzi*, the etiological agent of Chagas' disease, which represents a major cause of cardiomyopathy in Latin America where it affects around 8 million of people [1]. During its complex life cycle, the parasite encounters drastic environmental changes (*e.g.* in temperature and pH) and passes through several differentiation forms and two hosts, a reduviid insect vector (Triatomine) and a mammalian host. Trypomastigotes ingested by the insect vector with infected blood of the host differentiate into epimastigotes in the insect digestive tract [2]. These latter forms replicate in the insect midgut and later in the hindgut epimastigotes convert to metacyclic trypomastigotes, which are non-proliferative and infectious to human cells [3]. The latter differentiation process is known as metacyclogenesis and can easily be induced by submitting epimastigote cells to nutritional stress in triatomine artificial urine (TAU) medium and further by incubating in TAU medium supplemented with three amino acids and glucose (TAU3AAG) [4]. By the use of a metabolic stress, *in vitro* metacyclogenesis

Abbreviations: cAMP, cyclic AMP; AC, adenylyl cyclase; THT, trypanosome hexose transporter; TAU, triatomine artificial urine; VSG, variable surface glycoprotein.

* Corresponding author. Tel.: +55 21 39386756; fax: +55 21 22708647.
E-mail address: salmon@bioqmed.ufrj.br (D. Salmon).

http://dx.doi.org/10.1016/j.molbiopara.2015.04.002
0166-6851/

promotes a metabolic synchronization of the cells and thus allows analyzing both biological properties and gene expression of the cells at various stages of the differentiation. In *T. cruzi*, it was also reported that metacyclogenesis can be stimulated by adenylyl cyclase (AC) activators and cAMP analogues [5,6]. However, it is not clear yet whether the differentiation event induced by these soluble cAMP analogues is not merely due to their hydrolysis into AMP in the parasite, such as reported in the quorum sensing signalling pathway of *Trypanosoma brucei* [7,8]. Moreover, α-D-globin derived peptides from insect hindguts were postulated to promote metacyclogenesis through an AC stimulation event [9] but this stimulating effect on differentiation has not been reproduced so far using similar synthetic peptides [10]. It has been shown that before differentiation from epimastigotes to metacyclic trypomastigotes, cAMP levels increase three-to-four fold [11]. The presence of classical cycling nucleotide signalling in these organisms is still debated because the *T. brucei* PKA-like kinase is not activated by cAMP [12] but by cold-shock [13], contrary to the *T. cruzi* orthologue that was reported to be activated by cAMP [14]. Alternatively, several cAMP effectors (the cAMP response proteins CARP1 to CARP4) were identified in *T. brucei* by a genome-scale RNAi library screening [15], arguing for the presence of a putative novel cAMP signalling pathway in these parasites. Although it is clear that cAMP could play a major role in the development of trypanosomes, how cAMP synthesis is triggered and how it controls the cell cycle and/or differentiation is presently unclear. This probably results from the unusual mode of activation of these enzymes in trypanosomatids, for which the topological structure is highly different from this of their mammalians homologues. Indeed, the trypanosomal *AC* multigene family encodes many isoforms, which share a variable large extracellular N-terminal domain followed by a transmembrane helix and a conserved C-terminal catalytic domain [16,17]. Therefore, it was postulated that the activity of each of these isoforms is controlled by binding of a specific extracellular ligand to its receptor-like domain. Conversely, in *T. brucei*, it was shown that any stress that generates a membrane perturbation (*i.e.* acidic, thermal, proteolytic or osmotic stress) is sufficient to stimulate the AC activity of the parasite by dimerization of its catalytic subunits [18–20]. Interestingly, it was reported that AC could play a physiological role in regulating the osmoregulation through both the acidocalcisomes and contractile vacuole complex when the *T. cruzi* parasite is submitted to drastic changes in osmolarity [21] such as encountered during its development through the insect midgut [22]. It has been suggested that the significant cAMP increase observed during hyposmotic stress might occur by influx of ions, such as calcium [23], *via* a mechanosensitive channel and mediate the translocation of aquaporin from the acidocalcisomal membrane to the contractile vacuole complex, resulting in the water movement responsible for the volume reversal. Moreover, it was recently shown that AC activation during phagocytosis of lysing *T. brucei* by liver myeloid cells is responsible for inhibition of TNF-α synthesis through the activation of the protein kinase A of the host cells [24]. It was postulated that in these Salivaria extracellular parasites the function of AC at the host–parasite interface is probably linked to the specific expansion and diversification of their AC gene families encoding ~80 isoforms. This observation contrasts with intracellular trypanosomatids, such as *T. cruzi* and *Leishmania*, which only display a reduced number of these enzymes. Similarly to that shown in Salivaria trypanosomes [17,25,26], a *T. cruzi* AC gene fragment encoding the catalytic domain complements a *cya* deficient *Escherichia coli* mutant suggesting that its C-terminal domain is catalytically active [27]. Herein, we show that during the early stage of the *in vitro* metacyclogenesis, AC is transiently activated in a two-step process, as previously observed in *T. brucei* during the cellular differentiation from bloodstream into procyclic forms [28]. This observation suggests that AC activation can be achieved by metabolic stress. In parallel, by analyzing the expression pattern of AC isoforms, we show that expression of various AC is upregulated at the end of the metacyclogenesis. These data suggest that in response to a nutritional switching, the intracellular cAMP levels vary and lead to differential gene expression to allow the parasite to proceed though its life cycle.

2. Materials and methods

2.1. Growth and differentiation of parasites and isolation of nucleic acids

T. cruzi clone Dm28c [54] epimastigotes were cultured in liver infusion tryptose (LIT) medium [55]. *In vitro* metacyclogenesis of *T. cruzi* (Dm28c) was performed under chemically defined conditions as previously described [4]. Epimastigote parasites were harvested at saturation (5–7 days) and centrifuged at 1500 × *g* for 10 min at 4 °C, resuspended at 1×10^8 cells/ml in Triatomine Artificial Urine (TAU) medium (190 mM NaCl, 8 mM phosphate buffer, 17 mM KCl, 2 mM $MgCl_2$, pH 6.0), and incubated for 2 h at 37 °C. The parasites were then diluted to 5×10^6 cells/ml in TAU3AAG medium (TAU supplemented with 0.035% sodium bicarbonate, 10 mM L-proline, 50 mM sodium glutamate, 2 mM sodium L-aspartate and 10 mM glucose) and incubated for 72 or 96 h at 28 °C. The relative percentages of metacyclics/intermediate epimastigotes were determined by microscopic examination of parasites. Recovering of parasites at different stages of *in vitro* differentiation was carried out as previously described [56]. Total parasite DNA was extracted as described in [35]. Total parasite RNA was prepared following the LiCl-Urea method as previously described [57].

2.2. DNA and RNA analysis

The procedures employed for Southern and Northern blot hybridizations are described in [35]. Nucleic acids were blotted onto Hybond-N or Hybond-C Extra membranes (Amersham) and fixed following the manufacturer's instructions. Probes were labelled by random priming (Boerhinger) using [α^{32}P]dCTP (3000 Ci/mmol) (Amersham Pharmacia Biotech) and purified through a Sephadex G-50 column. Full-length DnaJ ORF corresponding to TcJ6 probe (1.05 kb PCR fragment), 5′-specific AC genomic probe (*Sal*I-*Sal*I, 0.75 kb) and α-tubulin cDNA probe (1.3 kb) were obtained as previously described [35]. TcrHT1 derived probe (0.3 kb) was obtained using the forward oligonucleotide: 5′-CAACTGACTGGCATCAATG-3′ and reverse oligonucleotide: 5′-GGACGGAAAGAGCGTGGGAA-3′ as primers for PCR amplification on Dm28c genomic DNA. The purified PCR fragment of 367 bp was cloned and sequenced. 5′ and 3′ specific AC derived probes were obtained by PCR amplification on genomic template (a 4.3-kb *Sal*I cl263g genomic subclone [35]) using, respectively, the oligonucleotides 5′-GGGCAGGCCGCATGCCCC-3′ and the reverse oligonucleotides 5′-GTTCATGATTGCGTGCACTAGTGC-3′ (DNA fragment of 2.683 bp corresponding to the entire N-terminal domain less the putative signal peptide) and the oligonucleotides 5′-CGTGACAACGAGAATGC-3′ and reverse nucleotide: 5′-CTCCCTGAAGCGCCTA-3′ (conserved catalytic fragment of 1.101 bp as described in Section 2.4). ssrRNA probe used as loading control in Southern analysis was obtained as previously described using the forward oligonucleotide: 5′-CGAACAACTGCCCTATCAGCC-3′ and the reverse oligonucleotide: 5′-CCTCATCTTTTTTTTTTGACATTGG-3′, as primers for RT-PCR on 5 μg of *T. cruzi* total RNA [38]. The α-tubulin probe was obtained from an incomplete cDNA of 1.3 kb sub-cloned in M13 [35]. Sequence analysis was performed using EMBOSS [58].

2.3. Pulsed-field gel electrophoresis

Chromosome separation (2×10^7 parasites/slot) was performed using the CHEF DRII (Biorad). Electrophoresis parameters were: 1% agarose, 450–850 s linear ramped pulse times, 144 h, 1.5 V/cm^{-1}, 0.5× TBE, 12 °C.

2.4. Expression of fragments of N-terminal domain and catalytic domain in E. coli and production of rabbit and mouse polyclonal antisera

An amino acid sequence alignment was first performed to find the fragment corresponding to the most variable region between the amino-terminal domains of ACs specific to the AC N-terminal domain from the Dm28c clone (ADC_Dm28c) (Fig. 1). To obtain this fragment as *E. coli* recombinant protein, two *BamH*I sites were created upstream and downstream of the amino-terminal fragment to insert the partial ORF (CYCNH2) into the *E. coli* expression vector PQE8 (Qiagen, Inc., USA). The N-terminal fragment was amplified by PCR using a *Vent* DNA polymerase (New England Biolabs) on a genomic template (Dm28c) using the forward oligonucleotide: 5′-GCGGATCCGGGCAGGCCGCATGCCCC-3′ and the reverse oligonucleotide 5′-AGGGATCCCACCCACGTACCACCGTC-3′ (*BamH*I sites are underlined). After PCR amplification and treatment by a *Taq* polymerase to add 3′ A-overhangs, the PCR fragment of 363 bp was subcloned into PCR2.1 (Invitrogen). The same strategy was used to clone the conserved catalytic AC C-terminal domain (CYCAT), which was amplified by PCR using as forward oligonucleotide: 5′-CGCGGATCCCGTGACAACGAGAATGC-3′ (*BamH*I site is underlined) and reverse nucleotide: 5′-CGAAGCTTCTCCCTGAAGCGCCTA-3′ (*Hind*III site is underlined) to produce a PCR fragment of 1.118 bp. The *BamH*I/*BamH*I and *BamH*I/*Hind*III fragments were subcloned, respectively, into *BamH*I/*BamH*I and *BamH*I/*Hind*III digested pQE8 (Qiagen, Inc., USA). The fusion construct was sequenced using flanking vector sequence as primers to ensure that the sequence derived from the *AC* gene was in the correct orientation and in frame with the 6× His tag. Expression of the recombinant protein was induced in *E. coli* strain M15 and cell lysates were prepared and analyzed by SDS-PAGE. The fusion product was purified on a Ni-nitrilotriacetic acid affinity column according to the manufacturer's instructions (Qiagen, Inc., USA). Polyclonal anti-CYCNH2 and anti-CYCAT antibodies were raised in rabbits immunized three times at 4 week intervals with 150 μg of pure recombinant protein. Polyclonal anti-CYCAT antibodies were raised in mouse immunized 4 times at 2 weeks intervals with 50 μg of pure recombinant protein. Rabbit antibody depletion on yeast lysate was performed by serial incubations with yeast acetone powder. Antibody specificity was checked by immunoblotting on whole bacterial protein lysate expressing recombinant proteins (data not shown) and *T. cruzi* protein extracts using as anti-rabbit IgG secondary antibodies conjugated to either AP or HRP (Supp. Fig. S2) or anti-mouse IgG secondary antibodies conjugated to HRP (Supp. Fig. S3).

2.5. Preparation of cellular extracts and immunoblotting

Total protein extracts of different stages of *T. cruzi* were prepared by washing the cells twice with ice-cold PBS and resuspending them in 1× Laemmli buffer [59] to a final concentration of 1×10^7 cells/μl. Proteins were separated by SDS-PAGE [59] and blotted onto Hybond-C Extra membranes (Amersham) following standard procedure. Blots were probed with anti-CYCAT and anti-CYCNH2 polyclonal antibodies (1/10,000 dilution) and a secondary HRP-conjugated goat anti-rabbit IgG (1/5000 dilution; Pierce) using enhanced chemiluminescence (ECL) for immunological detection following the manufacturer's instructions (Pierce). Monoclonal anti-GAPDH antibody [60] (1:5000) was used as internal loading control using a secondary HRP-conjugated goat anti-mouse IgG (1:5000 dilution; Pierce) for detection.

2.6. Immunofluorescence microscopy

Parasites were harvested by centrifugation and washed twice with PBS. Cells (5×10^7 ml^{-1}) were fixed directly on a polylysine treated slide by addition of an equal volume of formaldehyde in PBS (w/v, 3.5%) and incubated at room temperature for 2–3 min. The fixed cells were washed four times with TBS and permeabilized with TBS-Triton ×100 (0.1%) for 45 min. After blocking the cells with 5% BSA in TBS for 45 min at 37 °C, the parasites were washed twice with TBS and incubated with various concentrations of purified polyclonal anti-CYCAT antibodies in TBS containing 1% BSA overnight. The cells were washed twice with PBS and incubated with fluorescein isothiocyanate (FITC)-labelled anti-rabbit IgG secondary antibody (1/1000 dilution, Bioprobe) in the same buffer as used for primary antibody, for 45 min at 37 °C. The cells were washed three times with TBS and dehydrated serially in ethanol 70%, 85% and 96%. Finally, the slides were mounted with an anti-quench solution containing: diazabicyclo-octane (20 mg/ml), 80% glycerol and DAPI (0.1 μg/ml) to be viewed and photographed using a fluorescence microscope (Zeiss axioskop 2 coupled to a CCD camera) equipped with a digital *in situ* imaging system (ISIS 3).

2.7. Adenylyl cyclase assay and intracellular cAMP level measurement

Trypanosomes (3×10^7) were harvested by centrifugation at various times (0–96 h) of *in vitro* differentiation and resuspended in 1 ml of TAU buffer [4] and counted. Assays for AC were carried out on cells permeabilized by "swell dialysis" as previously described for *T. brucei* AC assay [42,43]. 3×10^7 cells were incubated 1 h at 4 °C in 100 μl of TES medium of low osmotic strength (50 mM KCl/5 mM $MgCl_2$/1 mM glucose/1 mM EGTA/20 μg/ml leupeptine/0.3 mM PMSF/13.3 mM TES, PH 7.5). After swell dialysis, sample of 10^7 cells (20 μl) were added to 80 μl of the assay cocktail (0.5 mM cAMP/10 mM phosphocreatine/50 units creatine kinase/1 mM EGTA/10 mM $MgCl_2$/20 mM KCl/0.5 mM ATP/20 μg/ml leupeptin/25 mM TES pH 7.5 and 1 μCi of [α^{32}P] ATP (10–40 Ci mmol^{-1}). The reaction was incubated for 5, 10 and 20 min at 27 °C and was stopped by adding 100 μl of stop solution (SDS 2%/ATP 40 mM/cAMP 0.01 M). cAMP was isolated according to Salomon et al. [61] by a two step chromatography and counted by liquid scintillation counting. AC activity was calculated by linear regression analysis of the rate of cAMP production. Each assay was performed in triplicate and various experiments were repeated with similar results.

Intracellular cAMP content was determined by colorimetric immunoassay kit following the instructions of the manufacturer (R&D Systems).

3. Results and discussion

3.1. Genomic characterization of T. cruzi AC subfamily associated to the THT locus

Because of the highly repetitive nature and hybrid content of the *T. cruzi* genome the exact size of the AC family is still not exactly defined but, based on published studies performed with cloned sequences [27,29,30], the genome assembly of the CL Brener strain (TriTrypDB release 4.1, http://www.tritypdb.org, 26 protein "hits" in both Esmeraldo-like and non Esmeraldo-like haplotypes), the shotgun sequencing performed on the Sylvio X10/1 strain [31] (28 "hits") and on the subspecies *T. cruzi marenkellei* [32], as well as studies performed by ourselves (Supp. Fig. S1) it can be estimated

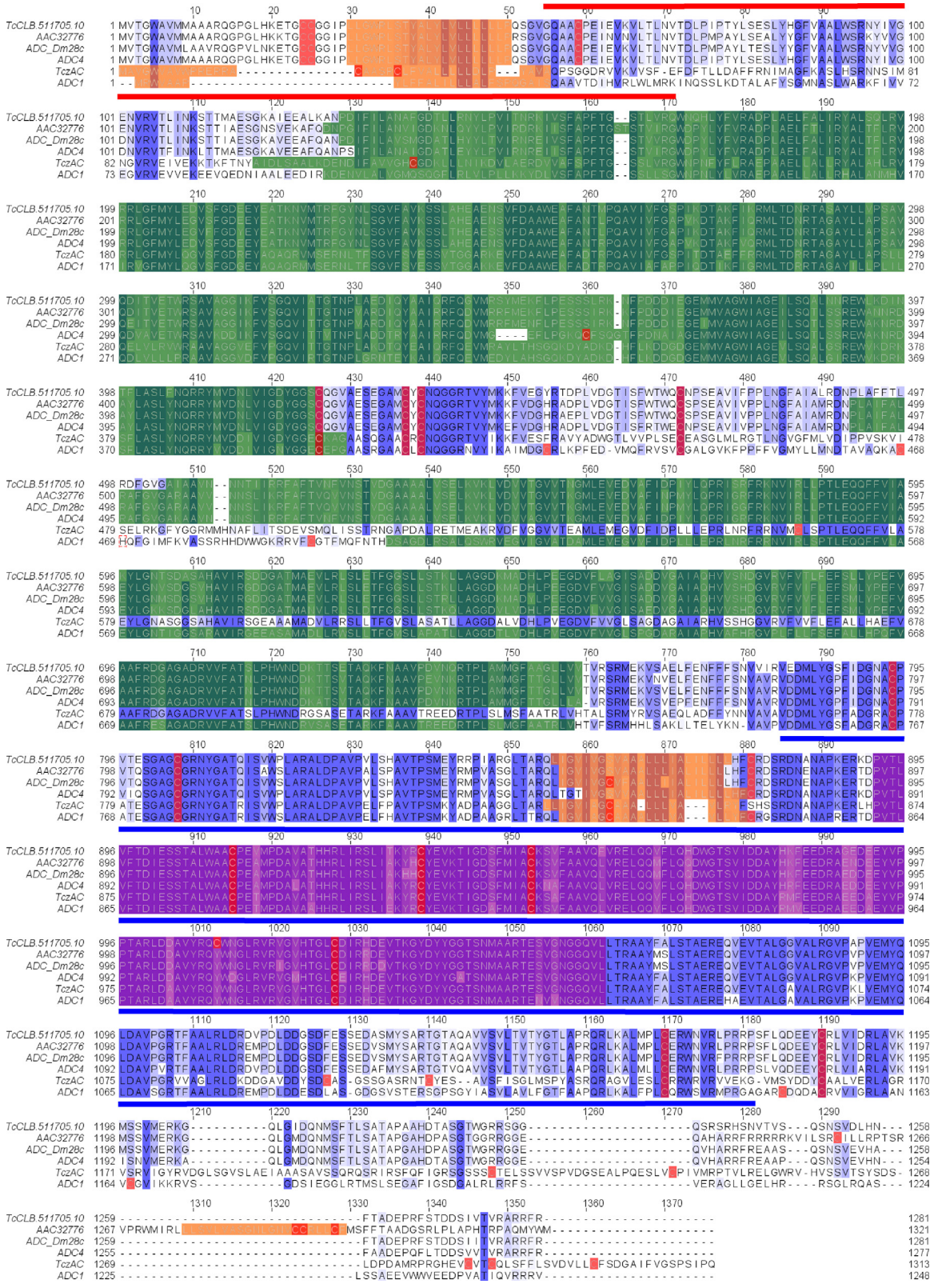

Fig. 1. Multiple amino acid sequence alignment of *T. cruzi* AC N-terminal domains. The following protein sequences were aligned using Clustal [62]: TcCLB.511705.10 from TriTrypDB; AAC32776: protein from GenBank entry AF031927 [29]; ADC_Dm28c: protein from GenBank entry JX861870 [35]; ADC4: protein from GenBank entry AJ011684 [27]; TczAC: protein from GenBank entry AF040382 [30]; ADC1: protein from GenBank entry AJ012096 [27]. Cysteines are coloured in red, SignalP (signal peptide) and TMHHH (transmembrane α-helix) motifs as detected by the InterProScan server [63] are coloured in orange, Nucleotidyl_cyc_III superfamily and Periplasmic_Binding_Protein_Type_1 superfamily motifs as detected by the NCBI CDD server [64] are coloured in magenta respectively green (note: for ADC1 the second PBP motif had an *E*-value of 0.08, for TczAC the second PBP motif could not be detected even with threshold of 100). The blue-scale (eventually overlayed on the other colours) expresses the % of identity (from dark to white: >80%, >60%, >40%, <40%). The red and blue lines mark, respectively, the N-terminal (CYCNH2) and C-terminal conserved catalytic (CYCOOH) domains used to generate specific antisera.

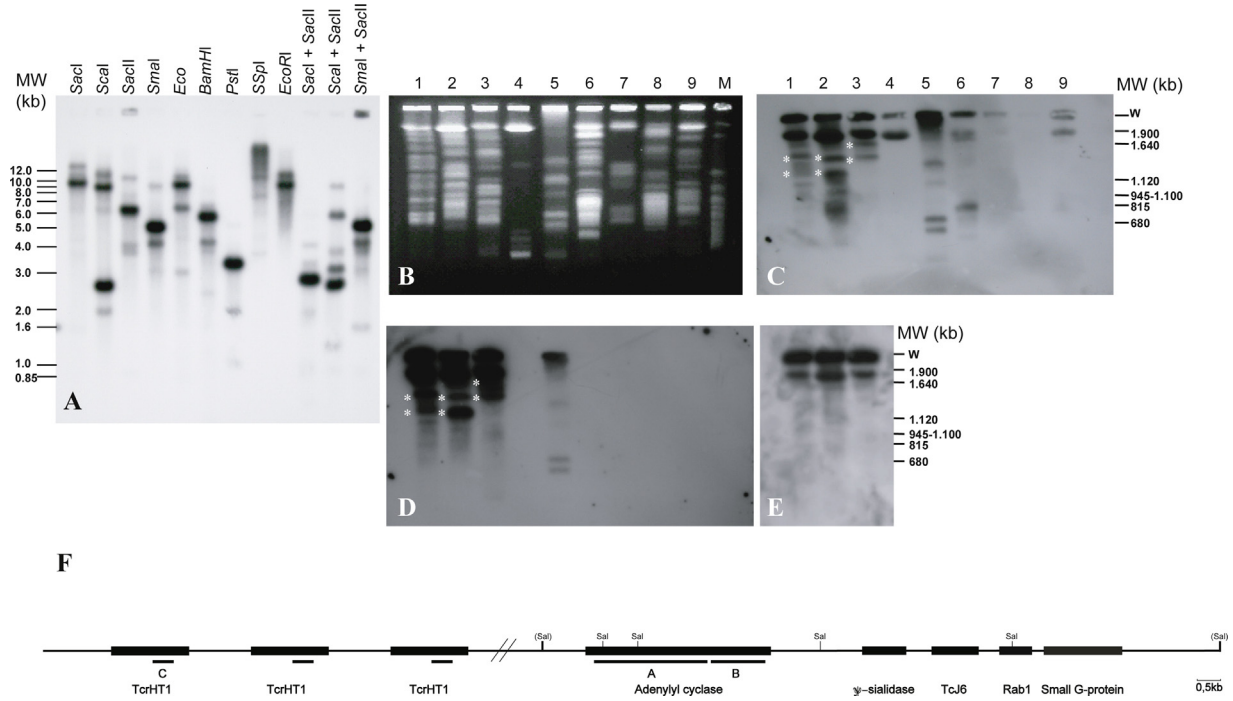

Fig. 2. Southern analysis and chromosomal location of the *TcTHTAC* gene subfamily in various trypanosomatid species. *Panel A*: genomic organization of the genes flanking the *AC* gene in a 14.3 kb *Sal*I fragment cloned from a genomic *T. cruzi* library from Dm28c [35]. *T. cruzi* (Dm28c) genomic DNA was digested with *Bam*HI, *Eco*RI (Eco), *Pst*I, *Sac*I, *Sac*II, *Sca*I, *Sma*I, *Ssp*I, *Sac*I + *Sac*II, *Sca*I + *Sac*II and *Sma*I + *Sac*II and analyzed by Southern blot hybridization with a 5′-specific AC fragment as PCR probe (probe A); *Panel B*: ethidium bromide staining of chromosomes from various trypanosomatids species separated by pulsed-field gradient gel electrophoresis and analyzed by Southern blot hybridization with various genomic PCR fragments. (1) *T. cruzi* Y strain, (2) *T. cruzi* CL Brener strain, (3) *T. cruzi* F strain, (4) clone 221a of *T. brucei stock* 427, (5) *T. rangeli* H14 strain, (6) *L. major* (7) *P. serpens*, (8) *H. m. muscarum*, (9) *C. fasciculata*; *Panel C*: hybridization using probe A corresponding to the AC N-terminal domain (2.6 kb), isoform-specific; *Panel D*: hybridization using probe B corresponding to the conserved AC catalytic domain; *Panel E*: hybridization using probe C corresponding to a conserved THT fragment (0.3 kb); *Panel F*: map and genomic organization of the genes flanking the AC gene in a 14.3-kb *Sal*I fragment cloned from a genomic Sau3A λEMBL3 *T. cruzi* library (cl263g) [35]; Sal, *Sal*I; Probes are represented by solid bars under the map; asterisks represent the chromosome pair labelled by both N- and C-terminal AC derived probes but not by THT probe; *S. cerevisiae* chromosomes were included as size standards (M) and W represents the well.

that the number of AC genes in the haploid genome is not much higher than 15. Among these putative ORFs, some are pseudogenes (2 and 4 pseudogenes for Esmeraldo-like and non Esmeraldo-like, respectively) or correspond to either N- or C-terminal domains that could be genuinely truncated genes or result from an incomplete coverage of the genome. Furthermore, contrary to its African homologue *T. brucei*, whose AC family reaches around 80 different members organized in several distinct sub-families (*ESAG*4 and *GRESAG* 4.1, 4.2, 4.3 and 4.4) [16,19,29,33,34], the *T. cruzi* AC family is much less complex and can be divided into two major subclasses (Fig. 1 and Supp. Fig. S1) located on at least six chromosomes: the TcADC1-like and TcADC4-like subfamilies [27]. Whereas the TcADC1-like subfamily contains genes organized as direct tandem repeats, the TcADC4-like, whose gene copies are spread out in the genome, can be subdivided into distinct groups, the bona fide TcADC4 located either at 5′ from the fatty acid elongase gene or at 3′ from the carboxypeptidase gene and the THT (trypanosome hexose transporter) locus associated AC isoforms (TcTHTAC) that intercalate inside a small syntenic block common to trypanosomatids species located downstream the cluster of glucose/hexose transporter genes [27,29]. In addition, the CLBrener genome contains a flagellar AC, named TczAC, which is not present in the tritrypDB, presumably because it falls into a gap in the genome assembly scaffold. Either it represents a unique member of a third family or it is a somewhat atypical member of the TcADC1-like family [30]. We previously mapped a polycistronic unit from Dm28c containing a genomic DNA fragment of 14.3 kb homologous to the region downstream of the THT genes cluster, which contains a full-length AC isoform (GenBank accession number JX861870) (Fig. 1 and schema in Fig. 2) [35]. The latter gene encodes a 1281 amino acids polypeptide (protein ID AFV95352) highly similar (92.4% identity) to the AC identified by Bringaud et al. (protein ID AAC32776) [29]. The primary amino acid sequence contains a highly conserved catalytic C-terminal domain (coloured in magenta in Fig. 1) and two conserved periplasmic binding-proteins type-1 (PBP type-1) located in the N-terminal domain (coloured in green). These domains might be involved in ligand-binding and transport similarly to the prokaryotic extracytoplasmic solute receptors (ESRs), which play a role in solute transport systems and chemotaxis [36]. It is interesting to note that several residues, including four cysteines, are found conserved in the linker region between the two PBP type-1 of the different *T. cruzi* AC isoforms, suggesting that the trypanosomal AC possibly assumes a similar folding of the extracellular domain [37]. By Southern blotting analysis, using a restriction enzyme cutting outside the gene (*Ssp*I in Fig. 2A) and a probe derived from the 5′ end of the gene and spanning the N-terminal domain less the signal peptide (probe A), in conditions of high-stringency hybridization, up to seven different gene copies were detected (Fig. 2A). This corresponds roughly to the number of ADC4-like genes found in the haploid genome of the CL Brener strain (TritrypDB, release 4.1). By using restriction enzymes, one cutting with a single site in the 5′ extremity of the ORF (*Sac*I) and one cutting with a single site in the 3′ extremity of the ORF (*Sca*I), no common fragment to both digests could be detected, confirming that the ADC4-like subfamily is not organized as a direct tandem repeat, as does the TcADC1-like subfamily, but is scattered throughout the parasite genome.

It was reported that the *T. cruzi AC* genes in the CL Brener strain were distributed over more than six different chromosomes [27] and the genome sequencing confirmed that *AC* genes are present

on chromosomes 2, 31, 35, 36, 37 and 39 in the two CL Brener haplotypes. Using a conserved probe derived from the catalytic domain (probe B), we observed a high chromosomal polymorphism of the *AC* gene family varying between various *T. cruzi* strains due to the high size-polymorphism of chromosomes between strains as well as some chromosome bands labelled in other related trypanosomatids species (Fig. 2C). Conversely, using a probe specific to the AC N-terminal domain (Fig. 2D, probe A), a similar pattern of chromosomal labelling was observed only for *T. cruzi* and *Trypanosoma rangeli* (note: in very low-stringency conditions of hybridization, small chromosomes of *Leishmania major* were also labelled, data not shown). By using a probe derived from a *THT* conserved region specific to the THT polycistronic unit TcrHT1, a comparable pattern of chromosomal bands in the megabase range were labelled in the three *T. cruzi* strains, except for one chromosomes pair, labelled by both N- and C-terminal AC derived probes that possibly correspond to the other ADC4-like (asterisks in Fig. 2C and D, probe C and data not shown). These results suggest that the upper chromosomal band recognized by the three probes corresponds to the THT associated ADC4-like AC cluster (chromosome 37 in CLBrener) while the two lower bands hybridizing with probe B (asterisks) are specific to the extra copies of ADC4-like ACs (chromosomes 2 and 35 in CLBrener). In addition, the TcTHTAC gene subfamily is specific to *T. cruzi*, although some homologous copies were found conserved in small chromosomes of *T. rangeli* and to a lesser extent *L. major* (data not shown). Taken together, these results suggest that during the evolution of the *T. cruzi* clade some *AC* gene have been secondarily inserted in the 3′ flanking region of the THT locus which forms a syntenic group of genes conserved in trypanosomatids [29]. These data supported the idea that AC gene expansion occurred independently in the different trypanosomatids species [24].

3.2. Expression of TcTHTAC subfamily during the metacyclogenesis

The expression pattern of TcTHTAC, as well as a 3′ flanking gene encoding the DnaJ protein (TcJ6 [35]) were determined during *in vitro* metacyclogenesis of *T. cruzi* by Northern blot analysis (Fig. 3A). Total RNA was extracted at various stages of the *in vitro* differentiation of *T. cruzi* epimastigotes and was analyzed with probes corresponding to the 5′ region of the *AC* gene, the *DnaJ* gene and the nuclear gene encoding the small subunit ribosomal RNA (ssrRNA), as a loading control for constitutively expressed genes [38]. Analysis of the relative intensities of the bands corresponding to the *AC* transcript and *ssrRNA* showed that the amount of the 3.9 kb mRNA increased during *in vitro* metacyclogenesis, reaching a maximum in metacyclic forms (arrow in Fig. 3A and data not shown). DNA probes corresponding to either *AC* (A) or *TcJ6* (B) genes recognized, apart from their individual mRNAs (arrows), the same high-molecular-weight transcript (sensitive to RNaseA DNase-free) (asterisk), which reached its maximum expression 24 h after the start of the differentiation (adhered forms). This suggests that the larger RNA species might be a common polycistronic precursor that upon processing (trans-splicing and polyadenylation) generates the respective mature mRNAs (metacyclic trypomastigotes). Using an alpha-tubulin probe as control a similar pattern was observed, however in this case different intermediate high-molecular mass RNA species were also detected (arrowhead), as already reported by Soares et al. [39]. This unusual detection of polygenic transcripts during the differentiation process possibly results from the inhibition of primary transcripts processing due to the metabolic stress applied to *T. cruzi* cells to differentiate them. This has already been described for the tubulin unit in heat shocked *T. brucei* cells, in which there was an accumulation of high-molecular-weight mRNA precursors containing both alpha- and beta-tubulin regions [40].

In order to investigate the AC protein expression in both epimastigotes and metacyclic trypomastigotes, we generated two different antisera to allow the discrimination between expression of the ADC4-like and the ADC1-like *T. cruzi* gene subfamily. Thus, specific polyclonal antibodies were produced against the isoform-specific N-terminal domain (anti-CYCNH2) or against the conserved catalytic domain (anti-CYCAT, Fig. 1) of the cloned version of Dm28c *AC*. Using the specific anti-CYCNH2 antiserum, we showed that in Western blot analysis of epimastigote cell extracts this antiserum recognized a narrow band corresponding to a polypeptide with an apparent molecular mass of around 146 kDa, similar to the molecular mass predicted from analysis of the primary polypeptide sequence of the Dm28c isoform (Fig. 3B). At the end of the differentiation, in the metacyclic infectious forms, the amount of AC detected was increased. Anti-CYCAT antiserum produced similar results although the bands appeared more intense and thicker, possibly due to the other AC isoforms recognized by the antiserum (Fig. 3B).

Taken together, these results showed that the expression of various ACs, including that of the TcTHTAC subfamily, is upregulated at the end of the metacyclogenesis and thus confirmed that the AC expression pattern is stage-specific, as previously suggested by De Castro et al. [41], who, by using an AC cytochemical substrate, detected by electron microscopy a plasma membrane labelling of higher intensity in trypomastigote cells than in amastigote or epimastigote cells.

Could the higher AC expression level detected in metacyclic cells be responsible for the 4-fold higher cAMP level observed in tissue culture derived trypomastigote cells *vs* epimastigote cells [11]? We attempted to address this question by measuring the basal AC activity *in vitro* during the differentiation process from epimastigotes to metacyclic trypomastigotes.

3.3. Time course of cAMP production, cellular adhesion and differentiation during in vitro metacyclogenesis

We have measured *in vitro* the activity of AC during metacyclogenesis using an *in situ* swell dialysis assay [42]. Two different stimulation phases were observed: a first activation phase occurring during the two first hours of nutritional stress and a second phase of stimulation between 6 and 48 h (Fig. 4A). The first enzymatic activation peak can easily be interpreted as a cell response to the metabolic stress that could trigger the activation of the parasite AC. To address if this increase of cyclase activity corresponds to an increase of intracellular cAMP we measured the total cAMP content of the cells submitted to nutritional stress (Fig. 4B). During the first hour of the differentiation event we observed a clear correlation between the increase of AC activity and the rise of intracellular cAMP content. Similarly, in *T. brucei*, it was shown that a mild acid environmental stress (pH 5.5) combined with a cold-shock (from 37 °C to 27 °C) can induce *in vitro* both the release of VSG and the activation of AC and trigger the cellular transformation of bloodstream to procyclic forms [28,43]. Regarding that several other mild environmental stresses have been shown to be involved in the simultaneous induction of VSG release and activation of AC (osmotic shock, Ca^{2+}, local anaesthetics, trypsin, PKC inhibitors [20]), it is not surprising that the *T. cruzi* AC could suffer a stimulation by metabolic stress. To explain how stress triggers functional AC activation it was hypothesized [44] that the catalytic activity of the trypanosomal AC could be actively prevented through inhibition of the dimerization of the C-terminal catalytic domain by an energy-dependent process, maybe involving a specific allosteric regulator site [18]. Either a general membrane perturbation, or the binding of specific ligands to the N-terminal PBP type-I domains, could relieve this inhibition and trigger activity [44].

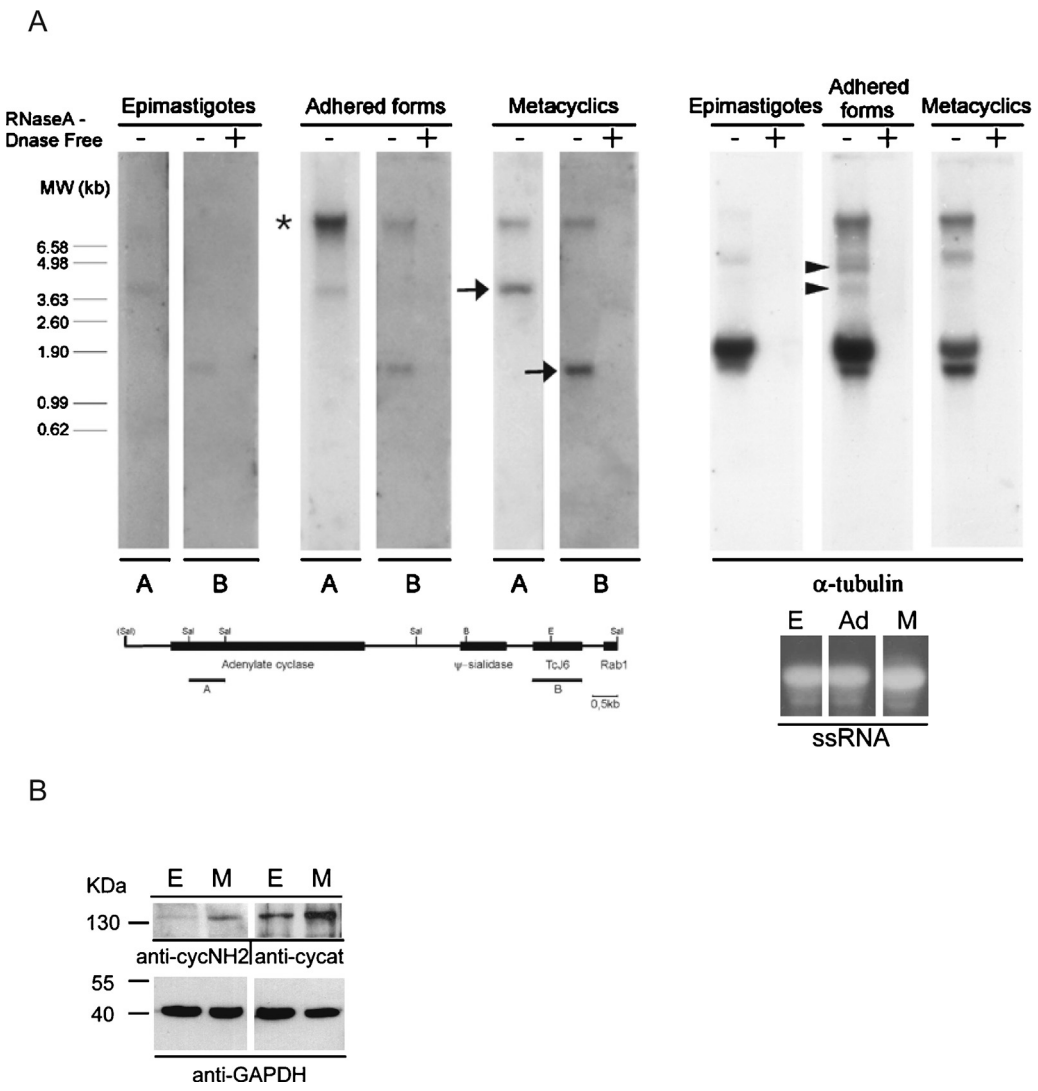

Fig. 3. Analysis of the expression pattern of AC during *in vitro* metacyclogenesis of *T. cruzi*. *T. cruzi* epimastigotes exponentially growing in complete medium (Epimastigotes) were subjected to a nutritional stress for 2 h in TAU medium and were then allowed to differentiate into complete TAU3AAG medium. 24 h after the start of the *in vitro* differentiation (adhered forms), most of the parasites were found adhered to the plastic culture flask, and the process was complete within 96 h to produce infectious metacyclic cells (metacyclics) [46]. *Panel A*: upregulated expression of AC mRNA during *in vitro* metacyclogenesis. 10 μg of total RNA was extracted at various stages of the *in vitro* differentiation of *T. cruzi* epimastigotes, treated or not with RNaseA DNase-free and was analyzed with probes for the *AC* gene (corresponding to the N-terminal domain) (A), *TcJ6* (DnaJ-like) gene (B) and *α-tubulin* and ssrRNA genes as loading controls. Analysis of the relative intensities of the band corresponding to the *AC* isoform transcript showed that the amount of the 3.9 kb mRNA increased during *in vitro* metacyclogenesis, reaching a maximum in metacyclic forms (arrow). A larger polycistronic RNA species (asterisk) recognized by both AC and TcJ6 probes was also detected reaching a maximum 24 h after the start of the differentiation. Arrowheads represent the accumulated high-molecular-weight precursors of the tubulin locus. The restriction map represents the genomic organization of the genes flanking the *AC* isoform gene associated to the *THT* locus in a 14.3 kb *Sal*I fragment cloned from a genomic *T. cruzi* library. Probes are represented by solid bars under the map. *Panel B*: Western blot analysis of the AC isoform expression in epimastigotes and metacyclic trypomastigotes. Total proteins from epimastigotes (E) and metacyclic trypomastigotes (M) were extracted from *T. cruzi*, respectively, in log phase or after *in vitro* metacyclogenesis (10^7 cells/lane), separated by SDS-PAGE in a 7.5% acrylamide gel, electroblotted and probed with either an anti-AC catalytic domain rabbit polyclonal antibody (anti-CYCAT) or an anti-N-terminal domain isoform-specific (anti-CYCNH2). Anti-GAPDH monoclonal antibody was used as a loading control.

The second phase of AC activity (6–48 h) corresponds to the cellular adhesion of epimastigotes to the plastic flask of the cell culture as shown by the decrease of the cell number in the supernatant (Fig. 4A), which is typically observed between 6 and 24 h of differentiation time [4]. However, the observation of a peak of adhered parasites occurring around 48 h after differentiation that corresponds to the second increase of intracellular cAMP content highly suggests a genetic link between cellular adhesion process and AC activation (Fig. 4B). This process of adhesion is also observed during metacyclogenesis of the parasite in the insect host when the epimastigotes adhere to the rectum cuticle to be differentiated into metacyclic cells and seems to be a prerequisite for the *in vivo* differentiation [45]. It is not clear how adhesion triggers the metacyclogenesis process but it has been shown that both adhesion and metacyclogenesis are triggered by nutritional stress *in vitro* [46]. The main differences observed during the first 24 h reside in the polypeptide profile, which is remodelled by the stage-specific expression of a battery of genes involved in the increase of resistance to the lysis mediated by the complement (starting after 6 h of differentiation) and expression of specific-metacyclic major surface antigens starting after 12 h of differentiation [47,48]. These observations led us to assess the expression profile of ACs during *in vitro* metacyclogenesis. Contrary to all expectations, the protein level of AC isoforms detected by the antibody decreased significantly upon metabolic stress and during the complete adhesion process (between 6 and 24 h), while in the free-swimming

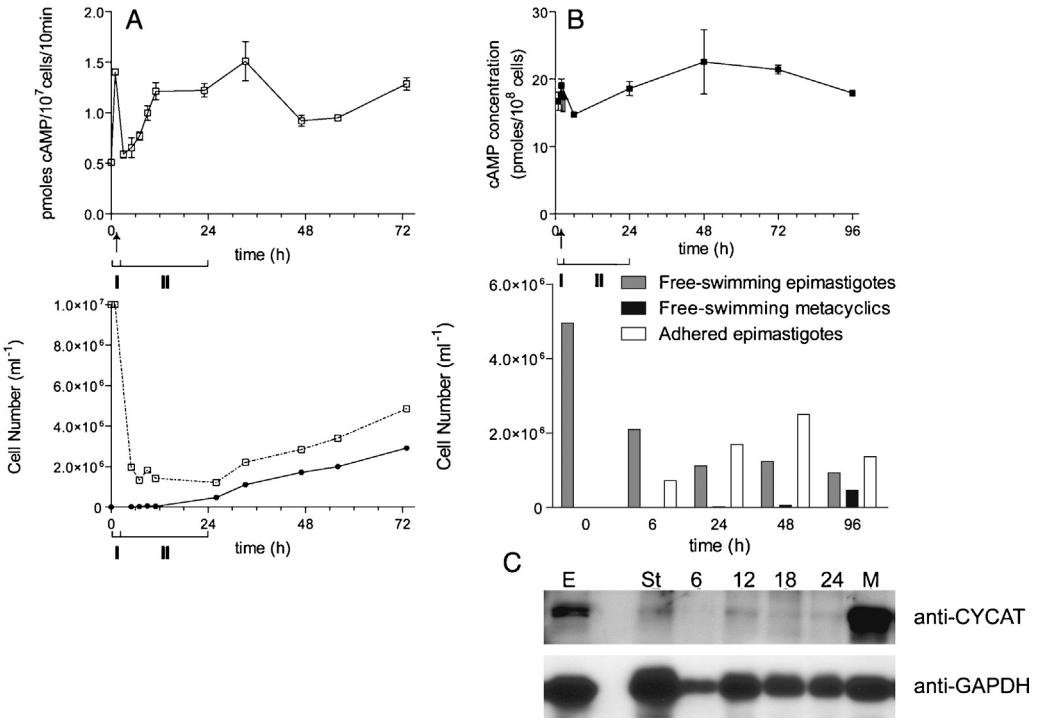

Fig. 4. Time course of AC activity *vs* cellular adhesion and differentiation (*Panel A*) and cAMP intracellular content *vs* cellular adhesion and differentiation (*Panel B*) during *in vitro* metacyclogenesis. Solid bars represent the nutritional stress (2 h) (I) and cellular adhesion (24 h) (II) time periods. Open squares and black circles represent, respectively, cell number of total free-swimming parasites and metacyclic trypomastigotes. Each value of cAMP synthesis (pmol/10^7 cells/10 min) and cAMP concentration represent the mean ± SE of three independent determinations. Western blot analysis of the AC expression during *in vitro* metacyclogenesis (*Panel C*). Total proteins from epimastigotes (E), E stressed for 2 h (St), adhered forms 6 h, 12 h, 18 h, and 24 h after differentiation (6, 12, 18, 24) and metacyclic trypomastigotes (M) were extracted from *T. cruzi*, respectively, in log phase or during *in vitro* metacyclogenesis (5×10^6 cells/lane), separated by SDS-PAGE in a 7.5% acrylamide gel, electroblotted and probed with either an anti-AC catalytic domain mouse polyclonal antibody (anti-CYCAT) or anti-GAPDH monoclonal antibody used as a loading control.

mature metacyclic forms the amount of AC attained its maximal expression (Fig. 4C). Because the expression level of the AC transcripts appeared higher in 24-h adhered forms than in log phase epimastigotes, we postulate that translational and/or post-translational controls are operating [49]. We also cannot discard the possibility that the decrease in immunoreactivity of the AC is due to some post-translational modifications, such as phosphorylation. In this respect, the presence of multiple putative phosphorylation sites that are conserved in the C-terminus of the ACs (including in the catalytic domain) may mask several epitopes recognized by the antibody raised against the catalytic domain when the residues are phosphorylated. In addition, it was reported that expression of few genes is switched on between 6 and 24 h of differentiation by a post-translational process of polysomal mobilization (reviewed in [47]). In this view, the second spike of stimulation of AC during the parasite differentiation might be involved in a cascade of activation of downstream effectors that could modulate key factors implicated in the regulation of the expression of some genes involved in biochemical processes triggering morphological transformations of *T. cruzi*. In addition, a PKA regulatory subunit was characterized in *T. cruzi* [14] whose expression is developmentally regulated and higher in trypomastigotes, similarly to that of TcTHTAC. Moreover, we did not see any correlation between the level of expressed enzymes and the basal AC activity or cAMP intracellular content at the end of the differentiation. This is not surprising in view of the fact that cAMP signalling involved in both cellular differentiation and proliferation processes is highly controlled in trypanosomatids [24,28,34]. The recent evidence of the presence of several insect-stage specific isoforms of flagellar AC in *T. brucei* [26] support the paradigmatic microdomain model involving compartmentalized cAMP production in space and time such as described in superior eukaryotes. Finally, these observations suggest that in response to a nutritional switching, the intracellular cAMP level varies and is correlated to the differential gene expression that allows the parasite to progress through its cycle.

3.4. *Localization of* T. cruzi *AC by indirect immunofluorescence*

The subcellular distribution of the *T. cruzi* AC family was determined by fluorescent microscopy, at two stages of parasite differentiation: dividing epimastigotes and quiescent metacyclic trypomastigotes. The anti-CYCAT antiserum (Fig. 5A–C) stained uniformly the plasma membrane of the epimastigote parasites, in addition some punctuated cytosolic distribution was also observed. Conversely, a different distribution of the trypanosomal protein was observed in metacyclic cells, where a high staining was seen at the level of the entire flagellum and the flagellar pocket (Fig. 5D–F). Although it was not possible to locate the ADC4-like by indirect immunofluorecence microscopy because of the very low antibody titre of the anti-CYCNH2 antiserum, based on the fact that anti-CYCAT antiserum recognized preferentially isoforms overexpressed in metacyclic forms such as ADC4-like members, we assume that very likely these isoforms locate in the flagellum. This redistribution of the localization of AC following differentiation is similar to that of the PKA regulatory subunit which locates on the plasma membrane and the flagellum in the trypomastigote forms and is distributed in the cytosol of the epimastigote forms [14]. Moreover, the preferential AC location on the parasite flagellum of metacyclic forms is in agreement with the observation reported by d'Angelo et al. [30] of the possible interaction of TczAC with the paraflagellar rod protein, component of the flagellar cytoskeleton. Similarly to *T. brucei* ESAG4 [42,50,51], the first trypanosomal AC having been reported to be located on the flagellum, TczAC was reported to be stimulated by calcium although

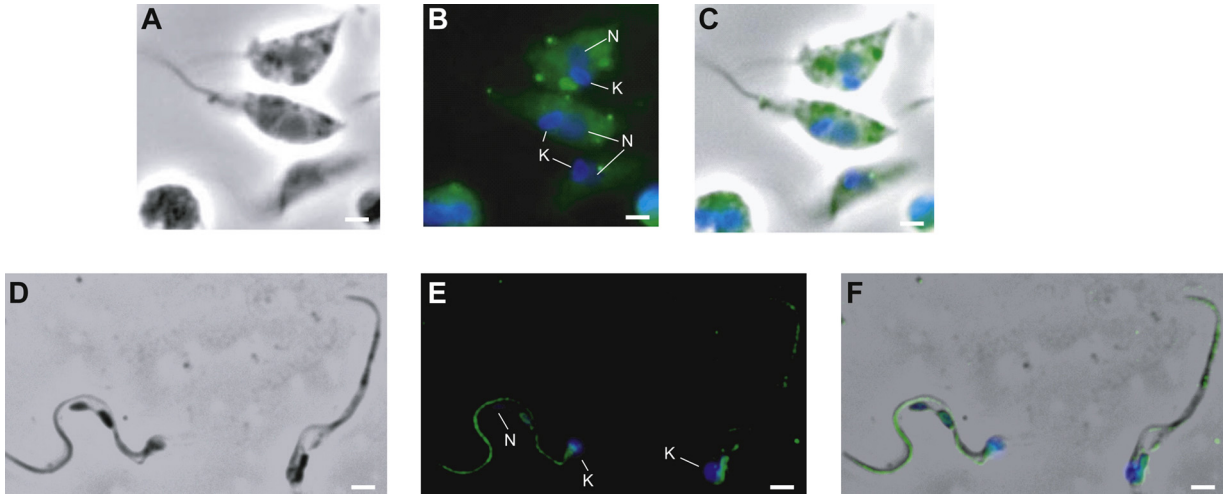

Fig. 5. Differential subcellular localization of AC in epimastigotes in the exponential phase of growth (*panel A*, *B*, *C*) and in metacyclic trypomastigotes (*panel D*, *E*, *F*) (clone Dm28c), determined by fluorescent microscopy. *A*, *D*: phase contrast images, *B*, *E*: merged fluorescent FITC and DAPI images and *C*, *F*: merged phase contrast and fluorescent images. Arrows indicate the position of kinetoplast (K) and nucleus (N) stained in blue by DAPI. The scale bars represent 2 nm.

by a non-physiological calcium range [30]. However the activation mechanism of both ESAG4 and TczAC by calcium is still unclear. Thus, if the existence of a cross-talk between the cAMP and calcium signalling pathways has been speculated [30], the general distribution of the trypanosomal AC (calcium dependent or not) over the flagellum could represent a most general adaptative mechanism allowing the parasite to sense quickly the changes of its environment and generate an appropriated response. The recent identification of several cAMP response proteins, including the two conserved eukaryotic flagellar proteins CARP2 and CARP4 (which possess an EF-hand domain located at its C-terminus end), supports this hypothesis [15]. The relevant characterization of a subset of *GRESAG4* of the *T. brucei* insect stage that regulates the social motility in the insect vector [52,53] revealed for the first time that cAMP signalling might control parasite social behavior.

Acknowledgments

This work was supported by a grant from the Conselho Nacional de Desenvolvimento Científico e Tecnológico (CNPq). We thank Sara Melville and Vanessa Leech from the University of Cambridge for providing the parasite DNA block of the 221a clone from *T. brucei stock* 427, Fernando Braga Stehling Dias for the help in checking the consensus of the nucleotide sequence of the AC gene, Michael Boshart (University of Munich, LMU) and Etienne Pays (Université Libre de Bruxelles, IBMM) for critical reading of the manuscript. A. H. was fellow of the Programa de Coordenação de Aperfeiçoamento de Pessoal de Nível Superior (CAPES) (Brazil), C. B. is a research fellow of CNPq (#304541/2012-5) and FAPERJ (#CNE E-26/102.775/2012).

Appendix A. Supplementary data

Supplementary data associated with this article can be found, in the online version, at http://dx.doi.org/10.1016/j.molbiopara.2015.04.002

References

[1] Rassi Jr A, Rassi A, Marin-Neto JA. Chagas disease. Lancet 2010;375:1388–402.
[2] Chagas C. Nova tripanozomiaze humana: estudos sobre a morfolojia e o ciclo evolutivo do *Schizotrypanum cruzi* n. gen., n. sp., ajente etiolojico de nova entidade morbida do homem. Mem Inst Oswaldo Cruz 1909;1:159–218.
[3] Brener Z. Biology of *Trypanosoma cruzi*. Annu Rev Microbiol 1973;27:347–82.
[4] Contreras VT, Salles JM, Thomas N, Morel CM, Goldenberg S. In vitro differentiation of *Trypanosoma cruzi* under chemically defined conditions. Mol Biochem Parasitol 1985;16:315–27.
[5] Gonzales-Perdomo M, Romero P, Goldenberg S. Cyclic AMP and adenylate cyclase activators stimulate *Trypanosoma cruzi* differentiation. Exp Parasitol 1988;66:205–12.
[6] Rangel-Aldao R, Triana F, Fernandez V, Comach G, Abate T, Montoreano R. Cyclic AMP as an inducer of the cell differentiation of *Trypanosoma cruzi*. Biochem Int 1988;17:337–44.
[7] Laxman S, Riechers A, Sadilek M, Schwede F, Beavo JA. Hydrolysis products of cAMP analogs cause transformation of *Trypanosoma brucei* from slender to stumpy-like forms. Proc Natl Acad Sci U S A 2006;103:19194–9.
[8] Mony BM, MacGregor P, Ivens A, Rojas F, Cowton A, Young J, et al. Genome-wide dissection of the quorum sensing signalling pathway in *Trypanosoma brucei*. Nature 2014;505:681–5.
[9] Fraidenraich D, Pena C, Isola EL, Lammel EM, Coso O, Anel AD, et al. Stimulation of *Trypanosoma cruzi* adenylyl cyclase by an alpha D-globin fragment from *Triatoma* hindgut: effect on differentiation of epimastigote to trypomastigote forms. Proc Natl Acad Sci U S A 1993;90:10140–4.
[10] Lara FA, Sant'anna C, Lemos D, Laranja GA, Coelho MG, Reis Salles I, et al. Heme requirement and intracellular trafficking in *Trypanosoma cruzi* epimastigotes. Biochem Biophys Res Commun 2007;355:16–22.
[11] Rangel-Aldao R, Allende O, Triana F, Piras R, Henriquez D, Piras M. Possible role of cAMP in the differentiation of *Trypanosoma cruzi*. Mol Biochem Parasitol 1987;22:39–43.
[12] Shalaby T, Liniger M, Seebeck T. The regulatory subunit of a cGMP-regulated protein kinase A of *Trypanosoma brucei*. Eur J Biochem 2001;268:6197–206.
[13] Kramer S [Dissertation] Characterization of a PKA-like kinase from *Trypanosoma brucei*. LMU München: Facultät für Biologie; 2005.
[14] Huang H, Weiss LM, Nagajyothi F, Tanowitz HB, Wittner M, Orr GA, et al. Molecular cloning and characterization of the protein kinase A regulatory subunit of *Trypanosoma cruzi*. Mol Biochem Parasitol 2006;149:242–5.
[15] Gould MK, Bachmaier S, Ali JA, Alsford S, Tagoe DN, Munday JC, et al. Cyclic AMP effectors in African trypanosomes revealed by genome-scale RNA interference library screening for resistance to the phosphodiesterase inhibitor CpdA. Antimicrob Agents Chemother 2013;57:4882–93.
[16] Pays E, Tebabi P, Pays A, Coquelet H, Revelard P, Salmon D, et al. The genes and transcripts of an antigen gene expression site from *T. brucei*. Cell 1989;57:835–45.
[17] Ross DT, Raibaud A, Florent IC, Sather S, Gross MK, Storm DR, et al. The trypanosome VSG expression site encodes adenylate cyclase and a leucine-rich putative regulatory gene. EMBO J 1991;10:2047–53.
[18] Bieger B, Essen LO. Structural analysis of adenylate cyclases from *Trypanosoma brucei* in their monomeric state. EMBO J 2001;20:433–45.
[19] Naula C, Schaub R, Leech V, Melville S, Seebeck T. Spontaneous dimerization and leucine-zipper induced activation of the recombinant catalytic domain of a new adenylyl cyclase of *Trypanosoma brucei*, GRESAG4.4B. Mol Biochem Parasitol 2001;112:19–28.
[20] Rolin S, Hanocq-Quertier J, Paturiaux-Hanocq F, Nolan D, Salmon D, Webb H, et al. Simultaneous but independent activation of adenylate cyclase and glycosylphosphatidylinositol-phospholipase C under stress conditions in *Trypanosoma brucei*. J Biol Chem 1996;271:10844–52.
[21] Rohloff P, Montalvetti A, Docampo R. Acidocalcisomes and the contractile vacuole complex are involved in osmoregulation in *Trypanosoma cruzi*. J Biol Chem 2004;279:52270–81.

[22] Kollien AH, Grospietsch T, Kleffmann T, Zerbst-Boroffka I, Schaub GA. Ionic composition of the rectal contents and excreta of the reduviid bug *Triatoma infestans*. J Insect Physiol 2001;47:739–47.
[23] Rohloff P, Rodrigues CO, Docampo R. Regulatory volume decrease in *Trypanosoma cruzi* involves amino acid efflux and changes in intracellular calcium. Mol Biochem Parasitol 2003;126:219–30.
[24] Salmon D, Vanwalleghem G, Morias Y, Denoeud J, Krumbholz C, Lhomme F, et al. Adenylate cyclases of *Trypanosoma brucei* inhibit the innate immune response of the host. Science 2012;337:463–6.
[25] Paindavoine P, Rolin S, Van Assel S, Geuskens M, Jauniaux JC, Dinsart C, et al. A gene from the variant surface glycoprotein expression site encodes one of several transmembrane adenylate cyclases located on the flagellum of *Trypanosoma brucei*. Mol Cell Biol 1992;12:1218–25.
[26] Saada EA, Kabututu ZP, Lopez M, Shimogawa MM, Langousis G, Oberholzer M, et al. Insect stage-specific receptor adenylate cyclases are localized to distinct subdomains of the *Trypanosoma brucei* flagellar membrane. Eukaryot Cell 2014;13:1064–76.
[27] Taylor MC, Muhia DK, Baker DA, Mondragon A, Schaap PB, Kelly JM. *Trypanosoma cruzi* adenylyl cyclase is encoded by a complex multigene family. Mol Biochem Parasitol 1999;104:205–17.
[28] Rolin S, Paindavoine P, Hanocq-Quertier J, Hanocq F, Claes Y, Le Ray D, et al. Transient adenylate cyclase activation accompanies differentiation of *Trypanosoma brucei* from bloodstream to procyclic forms. Mol Biochem Parasitol 1993;61:115–25.
[29] Bringaud F, Vedrenne C, Cuvillier A, Parzy D, Baltz D, Tetaud E, et al. Conserved organization of genes in trypanosomatids. Mol Biochem Parasitol 1998;94:249–64.
[30] D'Angelo MA, Montagna AE, Sanguineti S, Torres HN, Flawia MM. A novel calcium-stimulated adenylyl cyclase from *Trypanosoma cruzi*, which interacts with the structural flagellar protein paraflagellar rod. J Biol Chem 2002;277:35025–34.
[31] Franzen O, Ochaya S, Sherwood E, Lewis MD, Llewellyn MS, Miles MA, et al. Shotgun sequencing analysis of *Trypanosoma cruzi* I Sylvio X10/1 and comparison with *T. cruzi* VI CL Brener. PLoS Negl Trop Dis 2011;5:e984.
[32] Franzen O, Talavera-Lopez C, Ochaya S, Butler CE, Messenger LA, Lewis MD, et al. Comparative genomic analysis of human infective *Trypanosoma cruzi* lineages with the bat-restricted subspecies *T. cruzi marinkellei*. BMC Genomics 2012;13:531.
[33] Alexandre S, Paindavoine P, Hanocq-Quertier J, Paturiaux-Hanocq F, Tebabi P, Pays E. Families of adenylate cyclase genes in *Trypanosoma brucei*. Mol Biochem Parasitol 1996;77:173–82.
[34] Salmon D, Bachmaier S, Krumbholz C, Kador M, Gossmann JA, Uzureau P, et al. Cytokinesis of *Trypanosoma brucei* bloodstream forms depends on expression of adenylyl cyclases of the ESAG4 or ESAG4-like subfamily. Mol Microbiol 2012;84:225–42.
[35] Salmon D, Montero-Lomeli M, Goldenberg S. A DnaJ-like protein homologous to the yeast co-chaperone Sis1 (TcJ6p) is involved in initiation of translation in *Trypanosoma cruzi*. J Biol Chem 2001;276:43970–9.
[36] Tam R, Saier Jr MH. Structural, functional, and evolutionary relationships among extracellular solute-binding receptors of bacteria. Microbiol Rev 1993;57:320–46.
[37] Naula C, Seebeck T. Cyclic AMP signaling in trypanosomatids. Parasitol Today 2000;16:35–8.
[38] Fernandes AP, Nelson K, Beverley SM. Evolution of nuclear ribosomal RNAs in kinetoplastid protozoa: perspectives on the age and origins of parasitism. Proc Natl Acad Sci U S A 1993;90:11608–12.
[39] Soares CM, de Carvalho EF, Urmenyi TP, Carvalho JF, de Castro FT, Rondinelli E. Alpha- and beta-tubulin mRNAs of *Trypanosoma cruzi* originate from a single multicistronic transcript. FEBS Lett 1989;250:497–502.
[40] Muhich ML, Boothroyd JC. Polycistronic transcripts in trypanosomes and their accumulation during heat shock: evidence for a precursor role in mRNA synthesis. Mol Cell Biol 1988;8:3837–46.
[41] De Castro SL, De Souza W, Meirelles MN. Cytochemical localization of adenylate cyclase in the three developmental forms of *Trypanosoma cruzi*. J Protozool 1991;38:580–3.
[42] Voorheis HP, Martin BR. 'Swell dialysis' demonstrates that adenylate cyclase in *Trypanosoma brucei* is regulated by calcium ions. Eur J Biochem 1980;113:223–7.
[43] Rolin S, Hancocq-Quertier J, Paturiaux-Hanocq F, Nolan DP, Pays E. Mild acid stress as a differentiation trigger in *Trypanosoma brucei*. Mol Biochem Parasitol 1998;93:251–62.
[44] Pays E, Lips S, Nolan D, Vanhamme L, Perez-Morga D. The VSG expression sites of *Trypanosoma brucei*: multipurpose tools for the adaptation of the parasite to mammalian hosts. Mol Biochem Parasitol 2001;114:1–16.
[45] Boker CA, Schaub GA. Scanning electron microscopic studies of *Trypanosoma cruzi* in the rectum of its vector *Triatoma infestans*. Z Parasitenkd 1984;70:459–69.
[46] Figueiredo RC, Rosa DS, Soares MJ. Differentiation of *Trypanosoma cruzi* epimastigotes: metacyclogenesis and adhesion to substrate are triggered by nutritional stress. J Parasitol 2000;86:1213–8.
[47] Avila AR, Dallagiovanna B, Yamada-Ogatta SF, Monteiro-Goes V, Fragoso SP, Krieger MA, et al. Stage-specific gene expression during *Trypanosoma cruzi* metacyclogenesis. Genet Mol Res 2003;2:159–68.
[48] Contreras VT, Morel CM, Goldenberg S. Stage specific gene expression precedes morphological changes during *Trypanosoma cruzi* metacyclogenesis. Mol Biochem Parasitol 1985;14:83–96.
[49] Nardelli SC, Avila AR, Freund A, Motta MC, Manhaes L, de Jesus TC, et al. Small-subunit rRNA processome proteins are translationally regulated during differentiation of *Trypanosoma cruzi*. Eukaryot Cell 2007;6:337–45.
[50] Rolin S, Halleux S, Van Sande J, Dumont J, Pays E, Steinert M. Stage-specific adenylate cyclase activity in *Trypanosoma brucei*. Exp Parasitol 1990;71:350–2.
[51] Voorheis HP, Martin BR. Characteristics of the calcium-mediated mechanism activating adenylate cyclase in *Trypanosoma brucei*. Eur J Biochem 1981;116:471–7.
[52] Imhof S, Knusel S, Gunasekera K, Vu XL, Roditi I. Social motility of African trypanosomes is a property of a distinct life-cycle stage that occurs early in tsetse fly transmission. PLoS Pathog 2014;10:e1004493.
[53] Lopez MA, Saada EA, Hill KL. Insect stage-specific adenylate cyclases regulate social motility in African trypanosomes. Eukaryot Cell 2015;14:104–12.
[54] Contreras VT, Araujo-Jorge TC, Bonaldo MC, Thomaz N, Barbosa HS, Meirelles M de N, et al. Biological aspects of the Dm 28c clone of *Trypanosoma cruzi* after metacyclogenesis in chemically defined media. Mem Inst Oswaldo Cruz 1988;83:123–33.
[55] Camargo EP. Growth and differentiation in *Trypanosoma Cruzi*: I. Origin of metacyclic trypanosomes in liquid media. Rev Inst Med Trop Sao Paulo 1964;6:93–100.
[56] Bonaldo MC, Souto-Padron T, de Souza W, Goldenberg S. Cell-substrate adhesion during *Trypanosoma cruzi* differentiation. J Cell Biol 1988;106:1349–58.
[57] Pays E, Delronche M, Lheureux M, Vervoort T, Bloch J, Gannon F, et al. Cloning and characterization of DNA sequences complementary to messenger ribonucleic acids coding for the synthesis of two surface antigens of *Trypanosoma brucei*. Nucleic Acids Res 1980;8:5965–81.
[58] Rice P, Longden I, Bleasby A. EMBOSS: the European Molecular Biology Open Software Suite. Trends Genet 2000;16:276–7.
[59] Laemmli UK. Cleavage of structural proteins during the assembly of the head of bacteriophage T4. Nature 1970;227:680–5.
[60] Gradia DF, Rau K, Umaki AC, de Souza FS, Probst CM, Correa A, et al. Characterization of a novel Obg-like ATPase in the protozoan *Trypanosoma cruzi*. Int J Parasitol 2009;39:49–58.
[61] Salomon Y, Londos C, Rodbell M. A highly sensitive adenylate cyclase assay. Anal Biochem 1974;58:541–8.
[62] Larkin MA, Blackshields G, Brown NP, Chenna R, McGettigan PA, McWilliam H, et al. Clustal W and Clustal X version 2.0. Bioinformatics 2007;23:2947–8.
[63] Mulder N, Apweiler R. InterPro and InterProScan: tools for protein sequence classification and comparison. Methods Mol Biol 2007;396:59–70.
[64] Marchler-Bauer A, Zheng C, Chitsaz F, Derbyshire MK, Geer LY, Geer RC, et al. CDD: conserved domains and protein three-dimensional structure. Nucleic Acids Res 2013;41:D348–52.